NASA MEMO 4-11-59L

NASA MEMO 4-11-59L

IN-08
384 62

NASA

MEMORANDUM

LOW-SPEED STATIC STABILITY AND CONTROL CHARACTERISTICS

OF A MODEL OF A RIGHT TRIANGULAR PYRAMID

REENTRY CONFIGURATION

By John W. Paulson

Langley Research Center
Langley Field, Va.

NATIONAL AERONAUTICS AND
SPACE ADMINISTRATION
WASHINGTON
April 1959

NATIONAL AERONAUTICS AND SPACE ADMINISTRATION

MEMORANDUM 4-11-59L

LOW-SPEED STATIC STABILITY AND CONTROL CHARACTERISTICS OF A MODEL OF A RIGHT TRIANGULAR PYRAMID REENTRY CONFIGURATION

By John W. Paulson

SUMMARY

An investigation of the low-speed static stability and control characteristics of a model of a right triangular pyramid reentry configuration has been made in the Langley free-flight tunnel.

The investigation showed that the model had generally satisfactory longitudinal and lateral static stability characteristics. The maximum lift-drag ratio was increased from about 3 to 5 by boattailing the base of the model.

INTRODUCTION

An investigation is being conducted by the National Aeronautics and Space Administration to provide information on the stability and control characteristics from hypersonic to low subsonic speeds for configurations designed for lifting reentry from satellite orbit. The present investigation was made to provide some information at low subsonic speeds on the longitudinal and lateral stability characteristics of a model of a right triangular pyramid reentry configuration. This model was generally similar to the configuration of reference 1 which appears promising from a heat-transfer standpoint. The lower surfaces of the configuration have 45° dihedral and the upper surface is flat. The sweep of the leading edge in plan form was approximately 80°.

This study included static force tests to determine the longitudinal characteristics of the model erect and inverted at angles of attack from 0° to 60°, and tests to determine the lateral characteristics at constant angle of attack over a sideslip range from -20° to 20°.

Brief pitch and roll-control studies were made using a split-flap type of control at the rear of the model. Tests were also made to determine the effect on the longitudinal characteristics of boattailing the base of the model.

SYMBOLS

The lateral data are referred to the body system of axes (fig. 1) and the longitudinal data are referred to the stability system of axes. The origin of the axes was located to correspond to a longitudinal center-of-gravity position at 36 percent of the mean aerodynamic chord and to a vertical position approximately at the centroid of the cross-sectional area. The coefficients are based on the area of the particular configuration and the mean aerodynamic chord of the basic wing. (See table I.)

S	wing area, sq ft
$\bar{c}$	wing mean aerodynamic chord, ft
V	airspeed, ft/sec
b	wing span, ft
q	dynamic pressure, $\frac{\rho V^2}{2}$, lb/sq ft
ρ	air density, slugs/cu ft
β	angle of sideslip, deg
α	angle of attack of bottom of model (intersection of 45° dihedral surfaces), deg
L	lift, lb
D	drag, lb
F_L	lift force, lb
F_D	drag force, lb
F_Y	side force, lb
M_Y	pitching moment, ft-lb

M_X	rolling moment, ft-lb
M_Z	yawing moment, ft-lb
C_L	lift coefficient, F_L/qS
C_D	drag coefficient, F_D/qS
C_m	pitching-moment coefficient, $M_Y/qS\bar{c}$
C_n	yawing-moment coefficient, M_Z/qSb
C_l	rolling-moment coefficient, M_X/qSb
C_Y	lateral-force coefficient, F_Y/qS

$C_{n_\beta} = \frac{\partial C_n}{\partial \beta}$ per degree

$C_{l_\beta} = \frac{\partial C_l}{\partial \beta}$ per degree

$C_{Y_\beta} = \frac{\partial C_Y}{\partial \beta}$ per degree

APPARATUS AND MODELS

The model was tested in the Langley free-flight tunnel which is a low-speed tunnel with a 12-foot octagonal test section. A sting-type support system and an internally mounted three-component strain-gage balance were used.

The model was constructed of balsa. A three-view drawing of the model is presented in figure 2, and the dimensions are given in table I. Split-flap-type control surfaces having a 6-inch chord were added for some tests. In addition, for some tests these control surfaces were added at the rear of the model as extensions which could also be deflected to obtain a boattail effect. (See fig. 2.)

TESTS

Force tests were made to determine the static longitudinal and lateral stability and control characteristics of the model in the erect and inverted positions over an angle-of-attack range from 0° to 60°. The lateral characteristics were determined from tests made at various angles of attack over a sideslip range from -20° to 20°. The pitch and roll-control characteristics were studied using 10° deflection of several control configurations. Tests were also made to determine the effect on the longitudinal characteristics of boattailing the base of the model.

The tests were made at a dynamic pressure of 4.15 pounds per square foot which corresponds to airspeeds of 59 feet per second and a test Reynolds number of 1.17×10^6 based on the mean aerodynamic chord of 3.11 feet.

RESULTS AND DISCUSSION

Longitudinal Characteristics

The effect of pitch control on the longitudinal characteristics of the model is presented in figure 3. These data show that with 0° deflection of the pitch control the maximum lift coefficient occurred at an angle of attack of about 40° and the model was longitudinally stable up to this angle of attack. Deflecting the pitch control gave an almost constant increment in pitching moment up to an angle of attack of 40°. With the lower surface controls deflected, the angle of attack for maximum lift coefficient was increased to 45° and the model was stable to this angle of attack.

The longitudinal characteristics of the inverted model are presented in figure 4. It should be pointed out that the large difference in lift coefficient for a given angle of attack between these data and those for the erect model (fig. 3) is caused by the fact that the bottom of the model (intersection of the 45° dihedral surfaces) is used as the angle-of-attack reference while the lift is primarily dependent on the angle of attack of the flat upper surface of the model. These data show that the maximum lift coefficient for the inverted model is considerably higher than that for the erect model. The inverted model had about the same degree of longitudinal stability as the erect model (fig. 3) at the lower angles of attack, and the inverted model also became unstable at about the angle of attack (35°) for maximum lift.

The effect on the longitudinal characteristics of boattailing the base of the model is shown in figure 5. It is seen from these data that in the angle-of-attack range for $(L/D)_{max}$ the lift was not appreciably affected by boattailing but the drag was greatly reduced. This resulted in an increase in $(L/D)_{max}$ from about 3 to about 5.

Lateral Characteristics

The variation of C_Y, C_n, and C_l with β for various angles of attack is shown in figures 6 and 7 for the erect model and inverted model, respectively. These data are summarized in figure 8 in the form of the stability derivatives C_{Y_β}, C_{n_β}, and C_{l_β} plotted against angle of attack α. The values of the derivatives were obtained by measuring the slope between sideslip angles of 5° and -5°. Because of the non-linearity of the sideslip data (fig. 7), the derivative data for the model inverted are only useful in showing trends. The data of figure 8 show that the directional stability of the erect model becomes increasingly positive as the angle of attack increases while the inverted model has low positive or negative directional stability up to an angle of attack of 30° and then becomes very unstable. The variation of the effective dihedral parameter C_{l_β} with angle of attack α was not greatly affected by model attitude up to an angle of attack of 25°. At higher angles of attack the erect model had higher values of effective dihedral.

The data presented in figure 9 show that the rolling effectiveness of the configurations using lower surface flaps generally held up over the angle-of-attack range but these controls produced large adverse yawing moments. The upper surface control alone had favorable yawing moments but low rolling moments which decreased to zero at an angle of attack of about 45°. Control effectiveness was still obtained with control deflections of 10° from the 20° boattail surface.

Langley Research Center,
National Aeronautics and Space Administration,
Langley Field, Va., January 16, 1959.

REFERENCE

1. Cooper, Morton, and Stainback, P. Calvin: Influence of Large Positive Dihedral on Heat Transfer to Leading Edges of Highly Swept Wings at Very High Mach Numbers. NASA MEMO 3-7-59L, 1959.

TABLE I

DIMENSIONAL CHARACTERISTICS OF MODEL

Airfoil section	Wedge
Area, sq ft:	
Basic wing	3.96
Extensions added	4.76
20° boattail	4.67
Span, ft	1.76
Aspect ratio	0.78
Root chord, ft	4.67
Tip chord, ft	0
Mean aerodynamic chord, ft	3.11
Sweepback of leading edge, deg	79.4
Dihedral, deg	45
Control-surface chord, ft	0.5
Boattail extension, ft	0.5

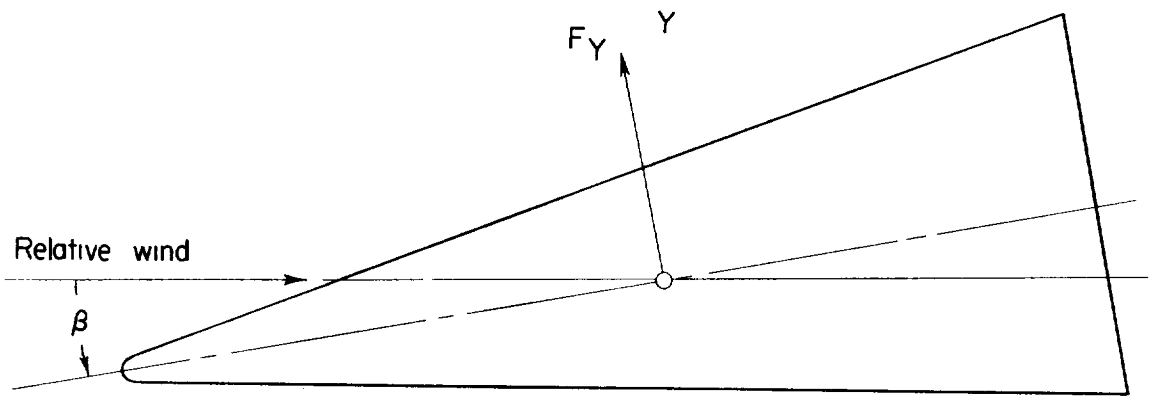

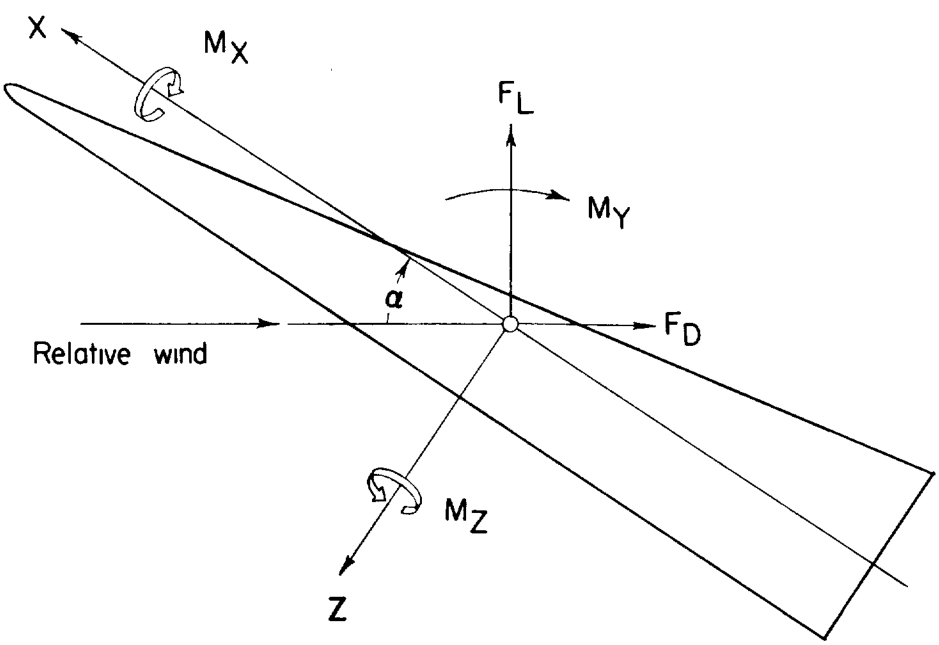

Figure 1.- Sketch of body-axis system showing positive direction of forces, moments, and angles.

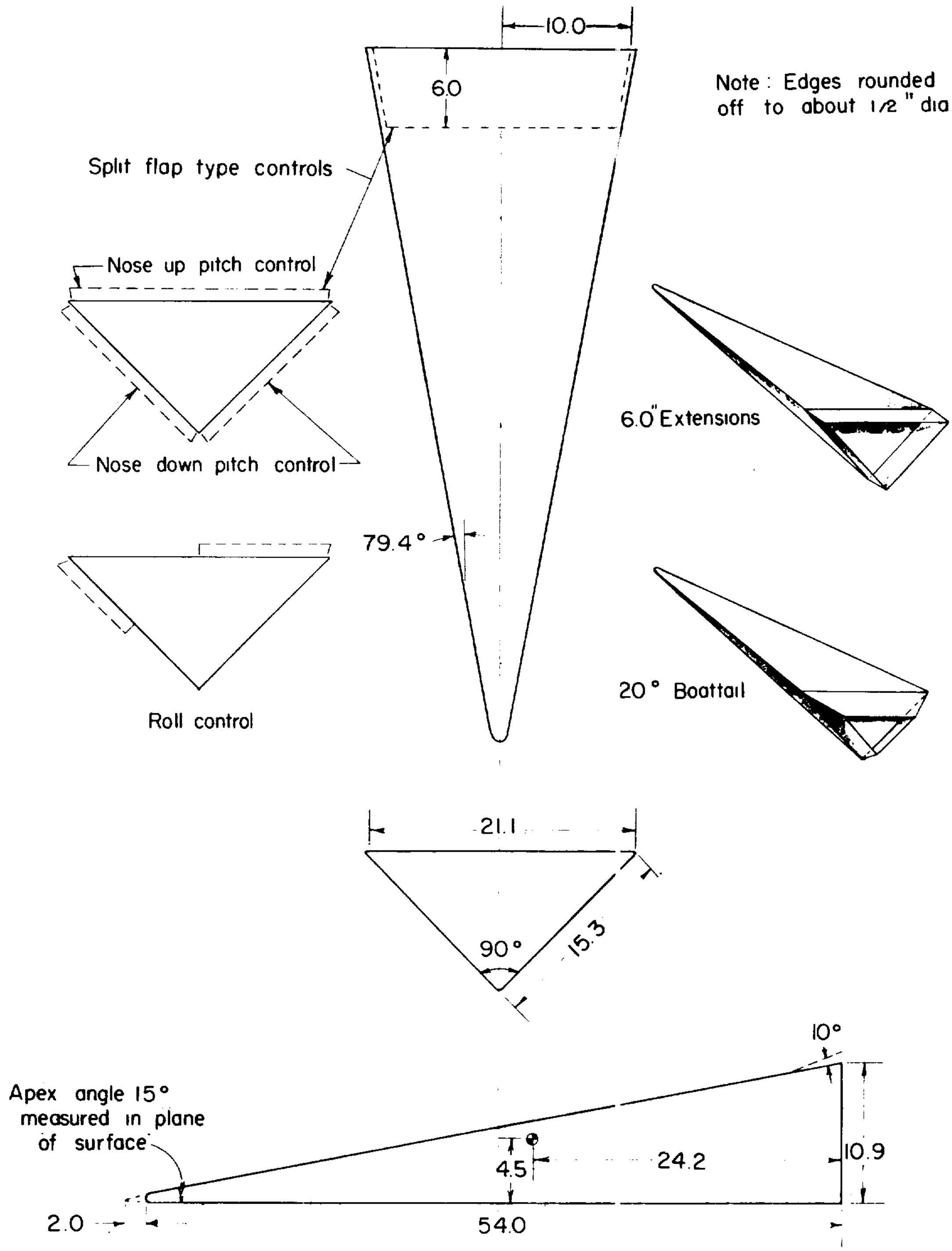

Figure 2.- Three-view drawing of model used in investigation. All dimensions are in inches.

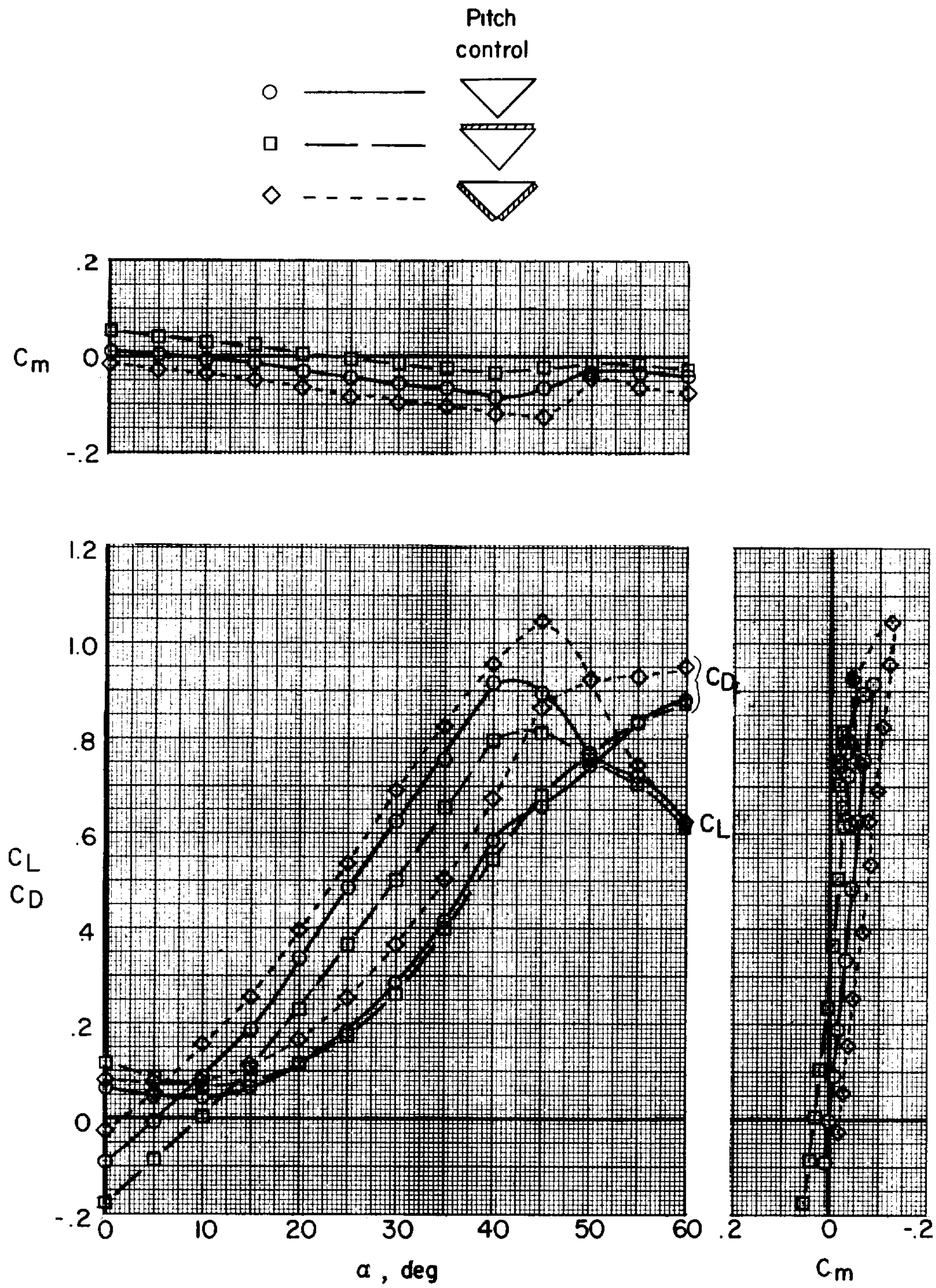

Figure 3.- Effect of pitch control on longitudinal characteristics of model. $\beta = 0^{\circ}$.

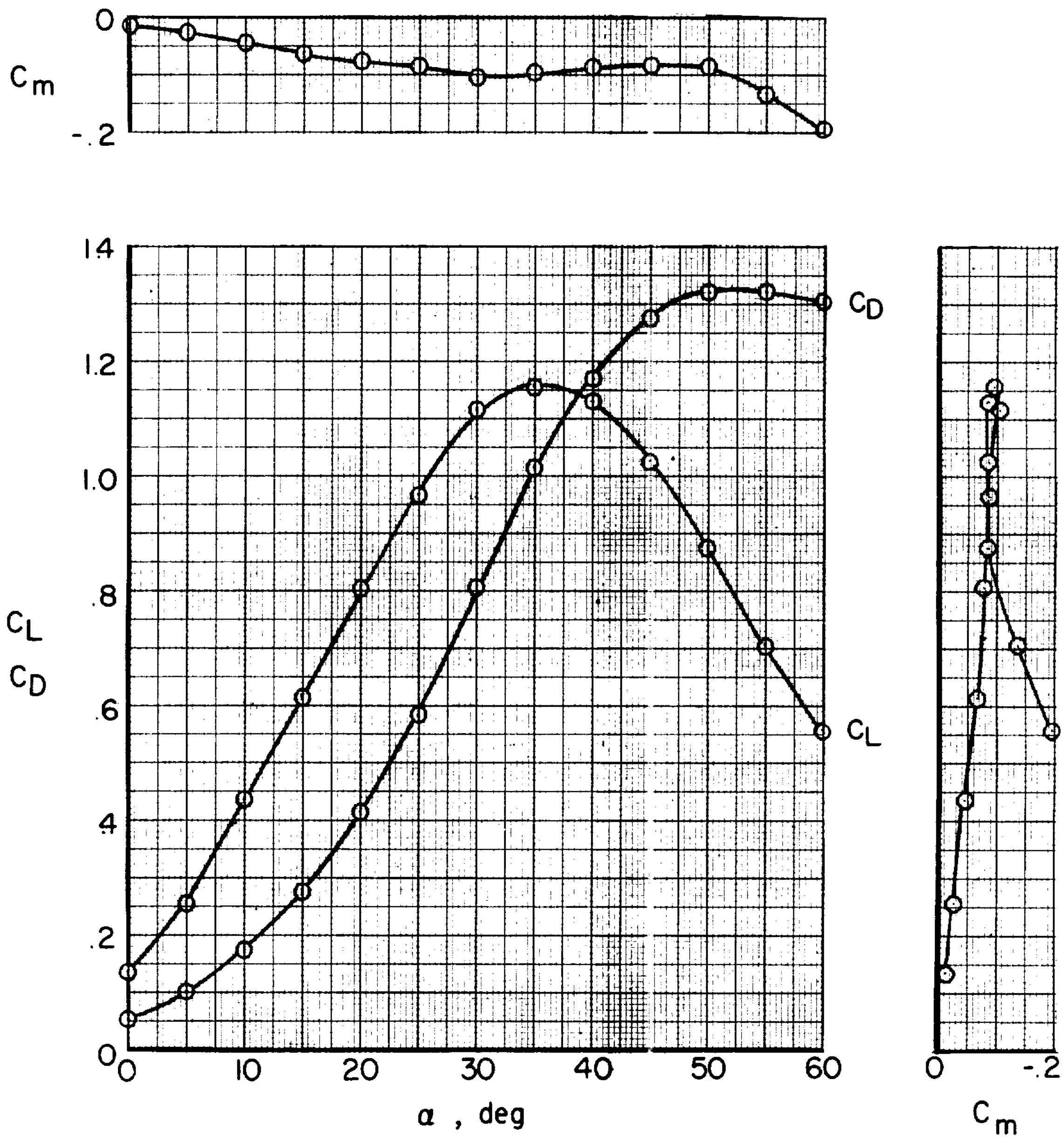

Figure 4.- Longitudinal characteristics of model in inverted position. $\beta = 0^{\circ}$.

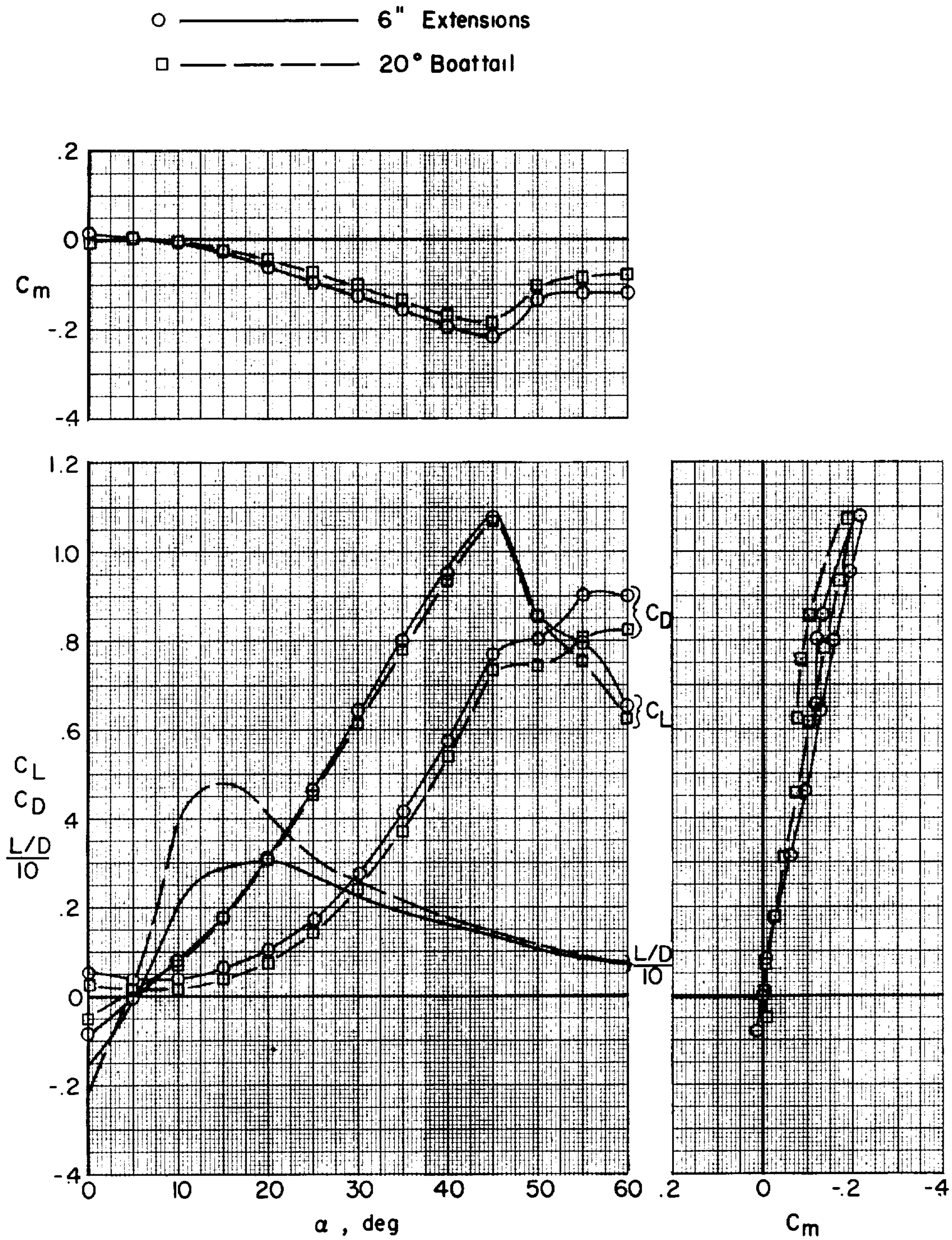

Figure 5.- Effect of boattailing on longitudinal characteristics of model. $\beta = 0^{\circ}$.

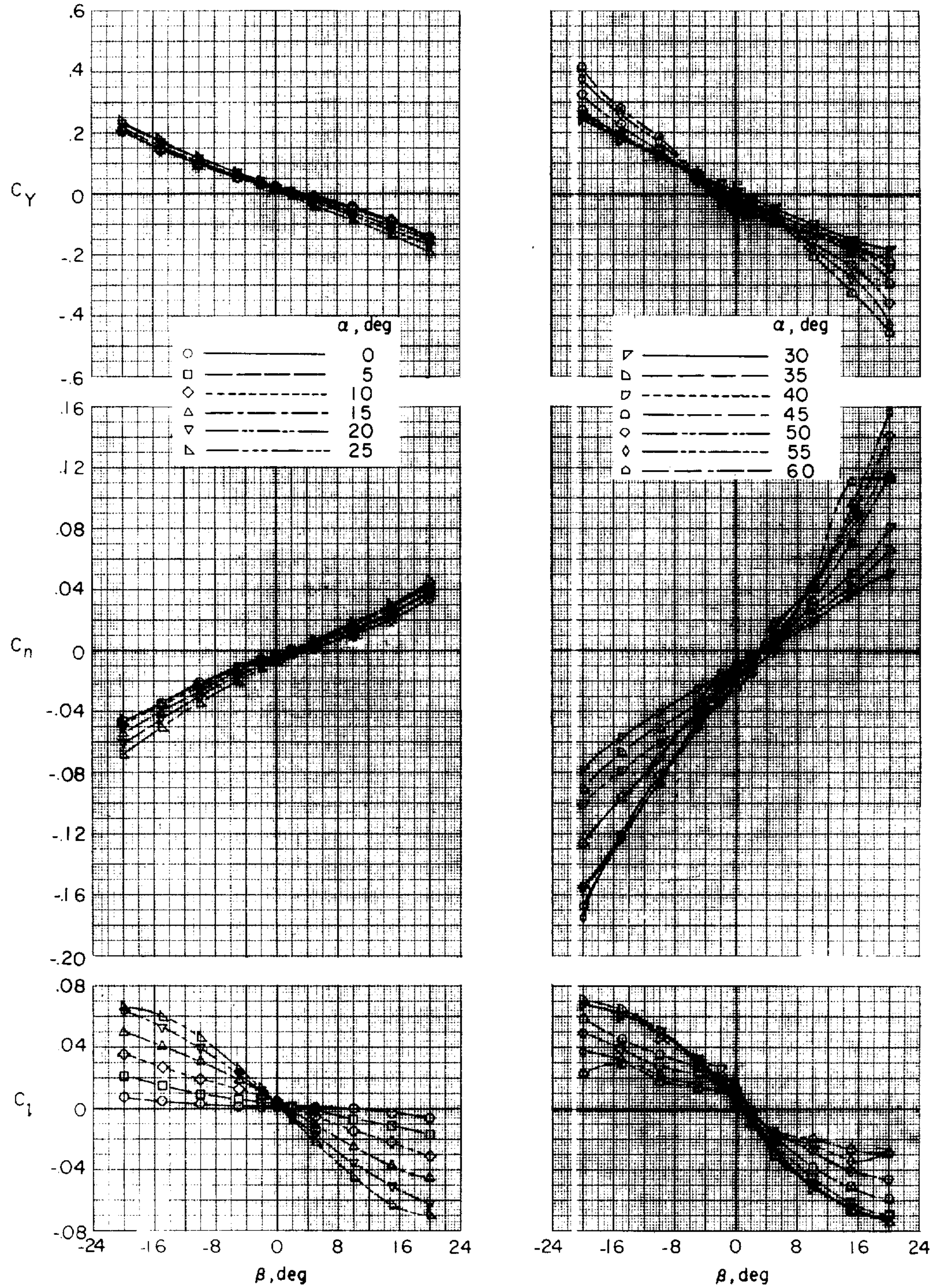

Figure 6.- Variation of static lateral stability characteristics of model with angle of sideslip. Controls undeflected.

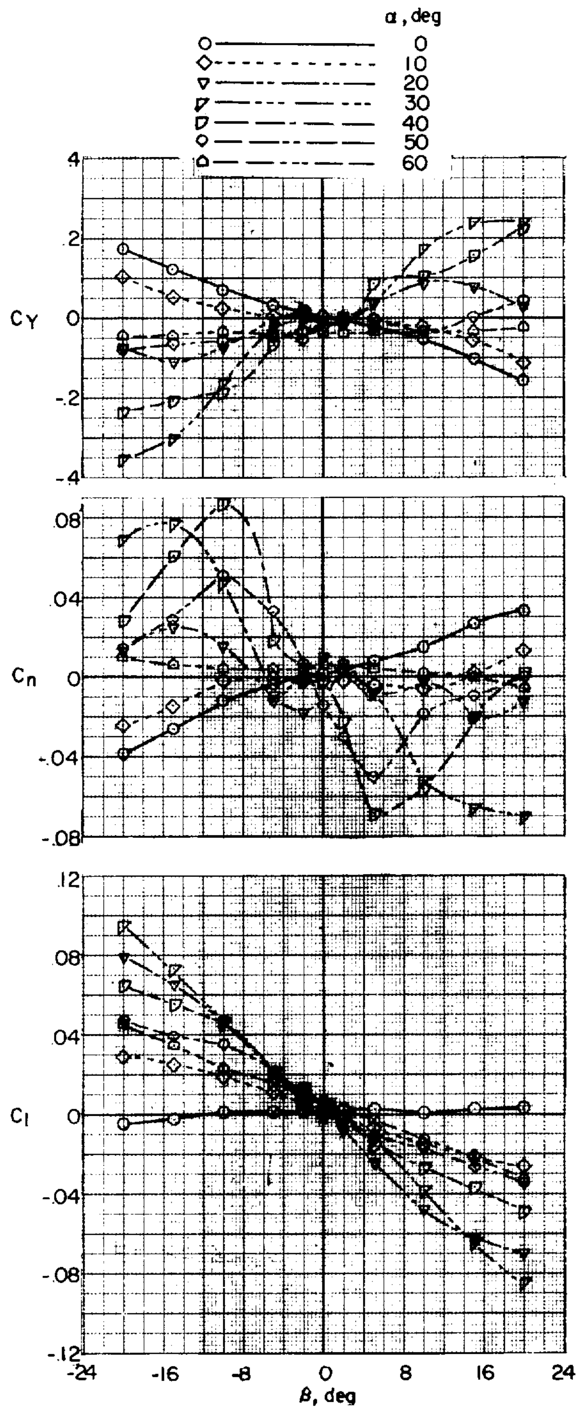

Figure 7.- Variation of static lateral stability characteristics of model with angle of sideslip. Model inverted. Controls undeflected.

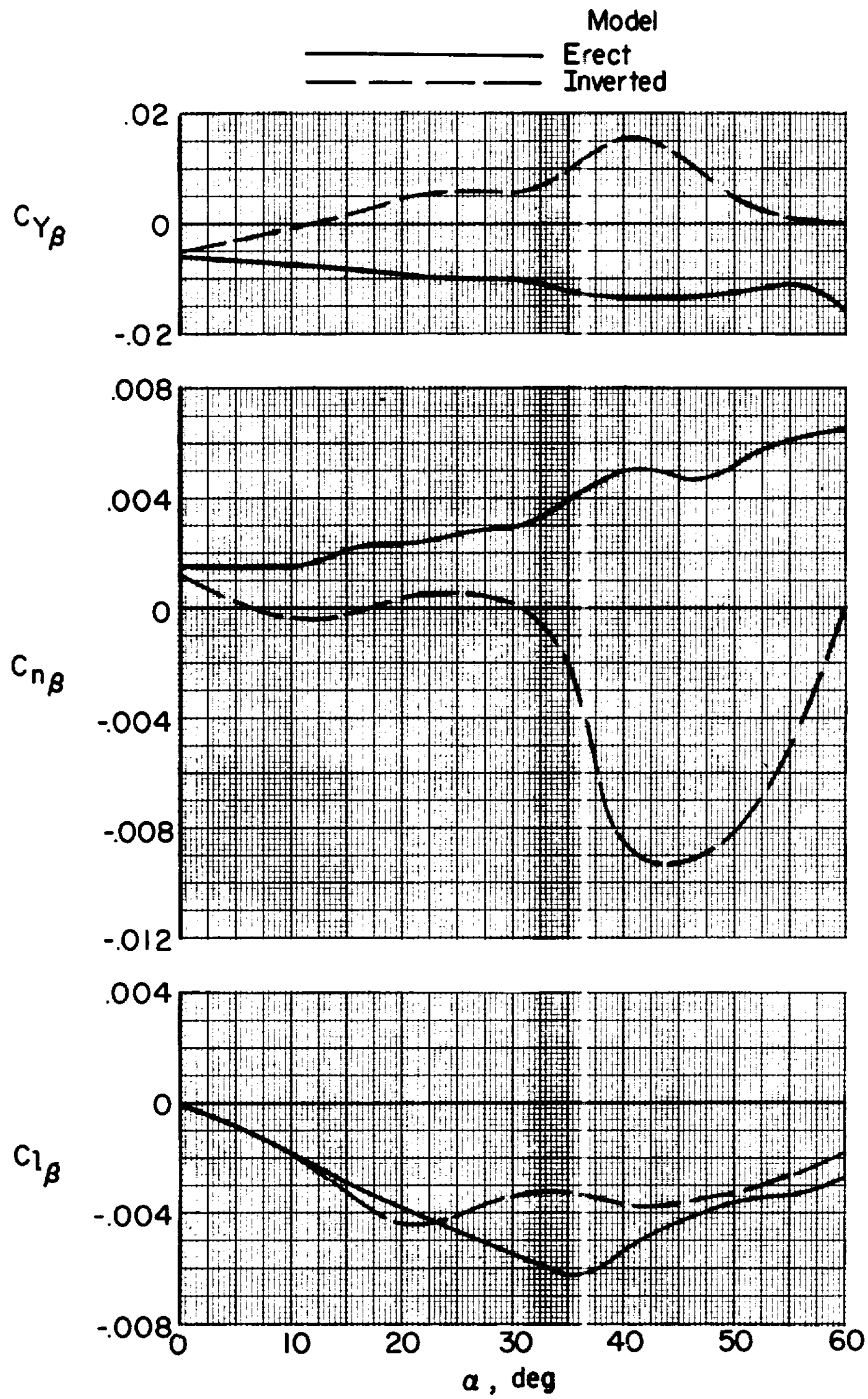

Figure 8.- Effect of model attitude on static sideslip characteristics. Controls undeflected.

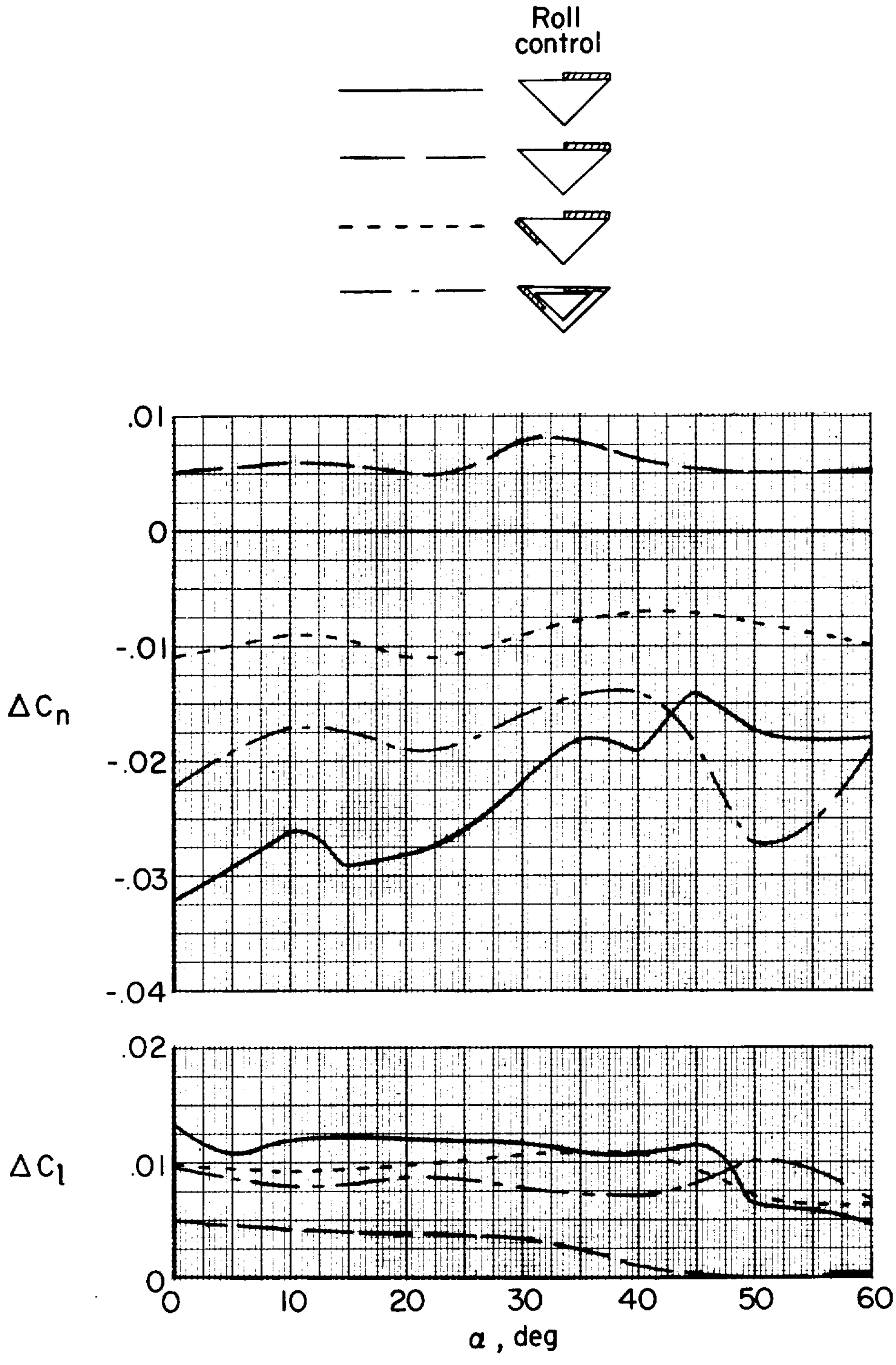

Figure 9.- Incremental yawing- and rolling-moment coefficients produced by various roll-control configurations deflected ±10°. $\beta = 0^{\circ}$.